Available online at www.sciencedirect.com

SciVerse ScienceDirect

www.elsevier.com/locate/matchar

Effect of the substrate temperature on the physical properties of molybdenum tri-oxide thin films obtained through the spray pyrolysis technique

H.M. Martínez[a], J. Torres[a,*], L.D. López Carreño[a], M.E. Rodríguez-García[b]

[a]Grupo de Materiales con Aplicaciones Tecnológicas, Departamento de Física Universidad Nacional de Colombia sede Bogotá, Colombia
[b]Departamento de Nanotecnología, Centro de Física Aplicada y Tecnología Avanzada, Universidad Nacional Autónoma de México, Campus Juriquilla, Querétaro, Qro., México, Colombia

ARTICLE DATA

Article history:
Received 23 March 2012
Received in revised form
1 September 2012
Accepted 6 November 2012

Keywords:
MoO_3
Spray pyrolisys
X-ray diffraction
Transmittance
Raman

ABSTRACT

Polycrystalline molybdenum tri-oxide thin films were prepared using the spray pyrolysis technique; a 0.1 M solution of ammonium molybdate tetra-hydrated was used as a precursor. The samples were prepared on Corning glass substrates maintained at temperatures ranging between 423 and 673 K. The samples were characterized through micro Raman, X-ray diffraction, optical transmittance and DC electrical conductivity. The species $MoO_3(H_2O)_2$ was found in the sample prepared at a substrate temperature of 423 K. As the substrate temperature rises, the water disappears and the samples crystallize into α-MoO_3. The optical gap diminishes as the substrate temperature rises. Two electrical transport mechanisms were found: hopping under 200 K and intrinsic conduction over 200 K. The MoO_3 films' sensitivity was analyzed for CO and H_2O in the temperature range 160 to 360 K; the results indicate that CO and H_2O have a reduction character. In all cases, it was found that the sensitivity to CO is lower than that to H_2O.

1. Introduction

MoO_3 is technologically appealing because of its optical and electrical properties. The material can crystallize in amorphous, alpha, and beta phases, or in a mixture of them. The alpha phase of the material crystallizes in a layered shape with covalent bonds inside the layers and weak bonds in between them; this allows the behavior of the electrons in the material to be considered as a bi-dimensional system. This phase is also interesting because other atoms and ions can be lodged in between layers, leading to the use of this material as an active element in Li batteries and in smart windows. MoO_3 has also been an active and passive component in solid-state electronics applications.

These applications require that the material has special structural, optical, and electrical characteristics, which depend on the preparation technique and on the quality of the precursor materials. Good-quality α-MoO_3 thin films are being produced through physical techniques such as high-vacuum thermal evaporation [1] and sputtering [2], techniques of great reproducibility with which electronic-grade materials are achieved. The chemical methods for producing MoO_3 thin films are low-cost technological options not requiring sophisticated equipment. Techniques such as spray pyrolysis [3], CVD [4], and sol gel [5] have shown interesting potential for producing good-quality materials. The spray pyrolysis technique has some advantages over the rest: low cost, easy implementation, and the possibility of coating large, variously-shaped areas.

The scientific community has devoted great effort to obtaining electronic-grade materials through chemical techniques, but a great deal of work is still needed. This paper

* *Corresponding author*. Tel.: +57 1 3165000x13067; fax: +57 1 3165135.
E-mail address: njtorress@unal.edu.co (J. Torres).
1044-5803/$ – see front matter
http://dx.doi.org/10.1016/j.matchar.2012.11.002

describes the influence of the substrate temperature on the physical properties of MoO_3 thin films prepared using spray pyrolysis from an ammonium molybdate tetra-hydrated precursor solution. A study of the samples' chemical composition and the substrate temperature's influence on their structural, optical and electric properties was carried out. Finally, the possibility of using this material as a gas sensor was evaluated.

2. Experimental Procedure

MoO_3 thin films were deposited using the spray pyrolysis technique from a 0.1 M solution of ammonium molybdate tetra-hydrated (Panreac) dissolved in distilled, deionized water. The samples were grown on corning glass substrates. Fig. 1 depicts a block diagram of the deposition equipment used. The substrates were located in the lower part of the reactor; the nozzle, in the upper part, moved horizontally with the help of a step motor and a position sensor. The molybdate solution was sprayed on the substrates using air at 4.9×10^4 Pa as a dragging gas. The separation between the nozzle and the substrates was 30 cm. The substrate temperature was controlled electronically with a tolerance of ±1 K. The reactor was protected by a Plexiglas box equipped with a gas extracting motor. The samples were prepared at different substrate temperatures, ranging between 423 and 673 K.

The substrates' area was 25×75 mm^2, and they were cleaned using the following procedure: they were soaked in soapy distilled water, rinsed with deionized distilled water, submerged for 24 h in a sulfochromic solution, rinsed with ultrasound in distilled, deionized water and then with ultrasound in alcohol, and then rinsed with acetone. Finally, the substrates were left to dry at ambient temperature.

The material deposited was characterized through X-ray diffraction measurements, SEM, Raman, optical transmittance in the visible spectrum, and DC electric conductivity measurements. The thin films were characterized through low-angle X-ray diffraction using a Philips X'Pert PRO PANalytical diffractometer with Bragg–Brentano geometry of monochromatic CuKα (λ = 1.54056 Å) radiation. The diffractograms were taken for a 2θ range between 10° and 70° at steps of Δ2θ = 0.05°, exposure time of 3 s, and skimming angle of 3°. The X-ray diffraction patterns were indexed using X' Pert High Score Plus software, which directly compares the experimental patterns with the data base of the Joint Committee of Powder Diffraction Standards (JCPDS), Inorganic Crystal Structure Data (ICSD).

Raman data were acquired on a Bruker Senterra dispersive Raman spectrometer equipped with a microscope, using a 785 nm laser and a 20× objective; the spectral resolution was 3–5 cm^{-1}. Laser power was varied between 50 and 100 mW, and 4–6 points were measured for each sample.

The morphological analysis of the samples was performed using a high-vacuum scanning electron microscope (HV-SEM, JSM 5600LV). These samples are made of non-conducting material; therefore, it was necessary to coat them with a layer of gold. The samples were fixed on the specimen holder with carbon tape and mounted on a copper specimen holder. The images were obtained with a secondary electron detector. The samples' optical characterization was carried out with a Varian 5000 spectrophotometer. The thickness of the samples was measured with a mechanical Veeco Dektak 150 Surface Profilometer with a tip diameter of 12.5 μm. A force of 10 μN was applied over the sample surface with a swept length of 3 mm for 100 s and a resolution of 0.100 μm. Two aluminum electrodes were deposited on the samples through high-vacuum (5×10^{-3} Pa) thermal evaporation in order to study their electrical behavior. The electrodes are comb-shaped, and are shown in the upper inset of Fig. 1. Two copper wires were affixed to these electrodes using LEIT-SILVER FLUKA silver tincture from BioChemika. The DC electrical conductance measurements and their sensibility to CO and H_2O were

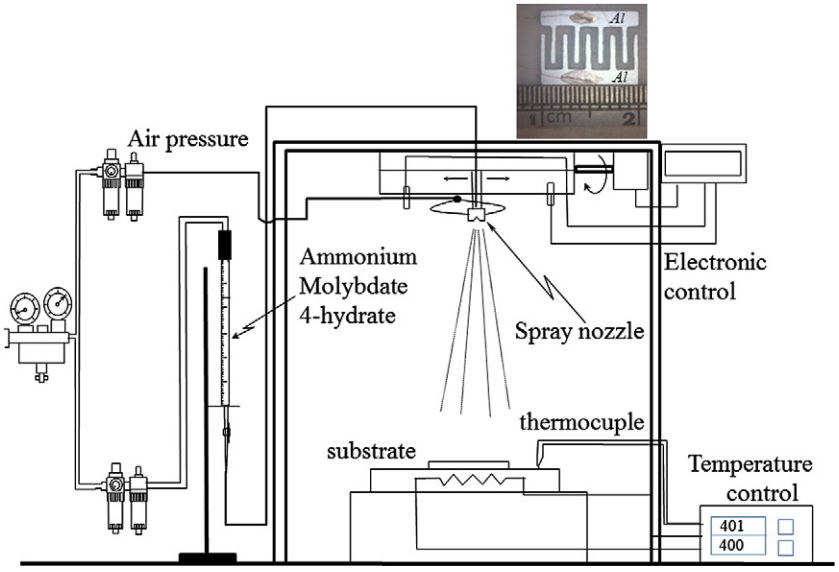

Fig. 1 – Diagram of the spray pyrolysis equipment used for films deposition. There are in the upper right part electrodes deposited for electrical measurements.

carried out in a high-vacuum system that routinely operates at a base pressure of 2×10^{-4} Pa. This equipment allows varying the samples' temperature in the range between 120 and 800 K; furthermore, it has a controlled gas admission system.

3. Results and Discussion

3.1. *Micro-Raman*

In Fig. 2, the micro-Raman spectra obtained for the samples prepared at different substrate temperatures are shown. From the figure, we can deduce that all the samples grown between 473 and 673 K show the same spectrum. The spectrum for the sample prepared at 423 K is clearly different from the others. Table 1, column 1, shows a summary of the bands' positions associated with the α-MoO_3 phase in accordance with the literature [6,7]. Column 2 shows the positions in cm^{-1} of peaks obtained for the samples prepared between 473 and 673 K. Comparing these two columns, it is clear that all the Raman bands of the samples prepared between 473 and 623 K agree with the data in the literature. The bands located at 665, 819, and 995 cm^{-1} stand out; these bands are characteristic of the orthorhombic α-MoO_3 crystalline phase. In the spectra there is no evidence of peaks associated with the β-phase. These results indicate that the samples prepared at substrate temperatures between 473 and 623 K crystallize in the α-MoO_3 phase.

The spectra for the sample prepared at 423 K (Fig. 2) was multiplied by 7 between 100 and 800 cm^{-1}. Column 3 in Table 1 shows the band positions obtained in this sample, and in column 4, the bands as given in the literature, associated with the bands of the MoO_3 $(H_2O)_2$ [6,8], especially the band at 953 cm^{-1}, are associated with the vibration mode ν(O=Mo), which is representative of MoO_3 $(H_2O)_2$. Comparison of the bands' positions in columns 3 and 4 indicates that the sample prepared at 423 K might be associated with the molybdenum oxide dihydrate.

Table 1 – Position comparison with the literature data of the micro-Raman peaks obtained for the samples.

α MoO_3 [7]	Ts=473 to 673 K	Ts=423 K	MoO_3 $(H_2O)_2$ [6]
115 (m)	115	115	119
129 (w)	127		
158 (m)	156		168
		179	184
198 (w)	197	201	
217 (w)	217	217	216
245	244		247
		262	
		268	272
283 (m)	284		
291	290		
337 (m)	337	341	331
365 (w)		366	353
379	377		
		386	386
			418
471 (w)			
			627
		571	
		654	
667 (w)	667		
		716	729
819 (vs)	819		
		848	
		898	
		907	
		923	934
		953 (vs)	952 [a]
995 (s)	995		

w=weak, m=medium, s=strong, vs=very strong.
[a] Oyerinde [8].

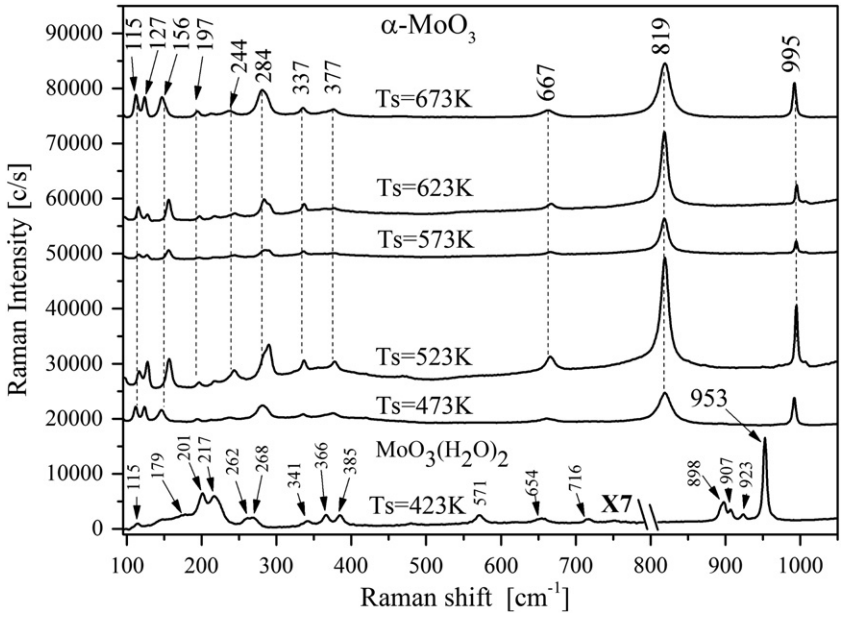

Fig. 2 – Raman spectra of samples prepared at different substrate temperatures. Results are compared with those of references [6,8].

3.2. *Structural and Morphological Characterization*

Fig. 3 shows the X-ray diffraction patterns obtained for the samples prepared at different substrate temperatures. All the samples exhibit polycrystalline phases. The X-ray diffraction patterns of the samples prepared at 473, 523, and 573 K have several peaks. As the substrate temperature rises to 623 and 673 K, the number of peaks is reduced and their intensity increases. From the indexation of the X-ray diffraction patterns it can be seen that for substrate temperatures of 473, 523, and 573 K the samples grow with differing preferential orientations. All the peaks are associated with the α-MoO_3, crystallographic card JCPDS, ICSD 05-0508. As the substrate temperature rises to 623 and 673 K, only peaks associated with the (0k0) planes appear in the patterns, indicating a preferential growth along direction [0k0] of the α-MoO_3. The intensity of the peaks increases, indicating an improvement of the crystalline structure of the material. This result is confirmed with the FWHM of the most intense peak (040), which is reduced as the substrate temperature increases in the samples prepared between 473 and 673 K.

In Table 2 the lattice parameters obtained on the samples prepared at substrate temperatures between 473 and 673 K are shown; also shown are the lattice parameters for the α-MoO_3 card ICSD 05-0508 and the values obtained by Bouzidi [3]. The presence in these samples of the MoO_3 orthorhombic phase (Fig. 3) is confirmed by the comparison of these parameters with the data in the crystallographic card (ICSD 5-0508). As the substrate temperature increases, the c parameter diminishes and the cell volume is also reduced, indicating that the crystalline structure of α-MoO_3 is improved with the rise of the substrate temperature.

The spectrum of the sample prepared at 423 K was indexed with the crystallographic card ICSD 01-088-1799 associated with the specie MoO_3 $(H_2O)_2$, indicating that the samples prepared at low substrate temperature are hydrated. This result was also confirmed with the Raman spectrum for the same sample. Fig. 4

Table 2 – Lattice parameters calculated for the sample prepared at different substrate temperatures (Ts). The values are compared with the data in JCPDS card ICDS 00-005-0508. (Tc crystallite size).

Ts (K)	*a* (Å)	*b* (Å)	*c* (Å)	Volume (Å^3)	Tc (nm)
473	3.922	13.811	3.878	210.06	17.03
523	3.944	13.778	3.782	205.52	18.28
573	3.945	13.812	3.783	205.37	17.08
623	3.959	13.724	3.738	203.37	31.08
673	3.984	13.778	3.667	201.28	43.81
	3.962	13.858	3.697	202.99	Card no. 00-005-0508
573	3.973	13.902	3.692	203.92	Bouzidi [3]

shows the evolution of the crystallite size and thickness with the substrate temperature. The crystallite size of the sample prepared at a substrate temperature of 473 K is around 18 nm, remains constant up to 623 K, and then grows to 40 nm at 673 K. The thickness of the samples prepared between 473 K and 573 K increases with substrate temperature, and then a reduction in the thickness is observed. This result can be interpreted in two ways: at high substrate temperatures, the material reaching the substrate is re-evaporated, making the sample thinner; on the other hand, the fact that the crystallite size increases and the thickness diminishes indicates that the crystallite size is growing laterally.

The previous results were corroborated through morphological analysis. Fig. 5 shows photographs of the samples' surfaces prepared at different substrate temperatures. The magnification used for all samples was 500×. It can be observed in the photographs that samples prepared at low temperatures have regular and flat surfaces, and the material shows a layered or terrace-like growth. This magnification does not clearly show grain borders, indicating that if grains exist, their size is too small, or the energy supplied to the sample does not allow nucleation processes. Surfaces of

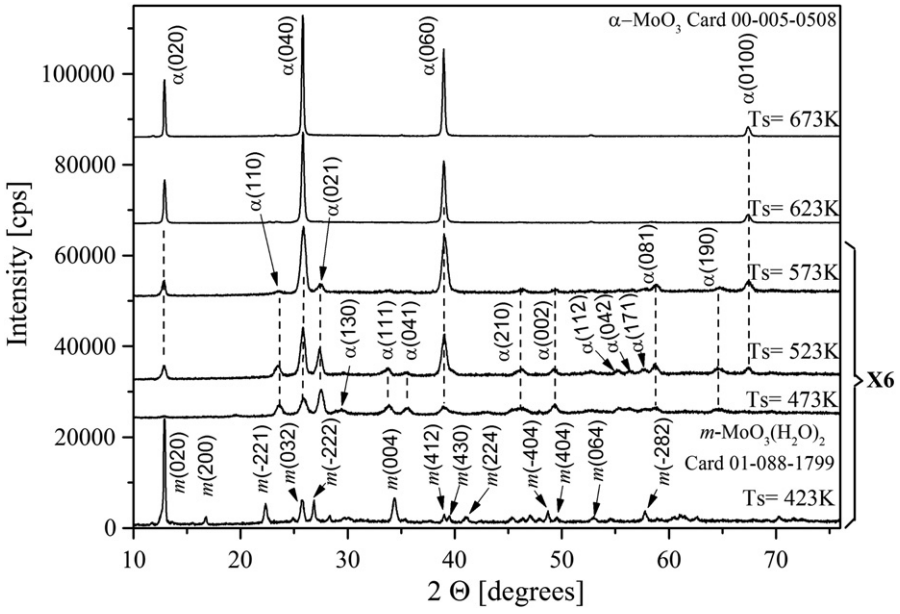

Fig. 3 – X-ray diffraction spectra from samples prepared at different substrate temperature (Ts): 423, 473, 523, 573, 623 and 673 K.

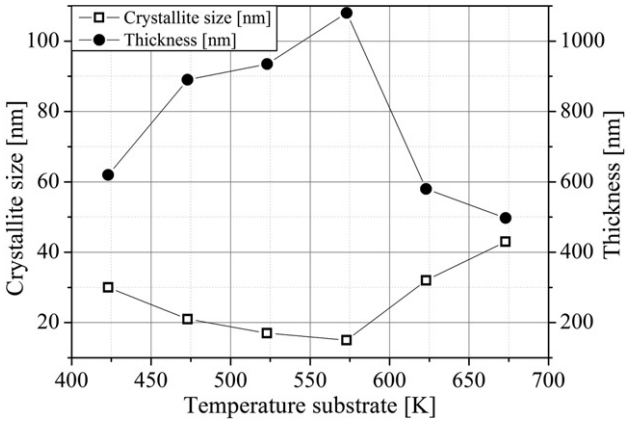

Fig. 4 – Variation of crystallite size and film's thickness with substrate temperature.

samples prepared at 473 K show initial formation of the material's chains growing on the flat surface of the material. These chains have a circular form and interlocking loops; the width of the chains is about 0.5 μm, and the diameter of the circle formed is on the order of 10 μm. When the temperature increases, the surface density of the chains increases and they lose their circular shape. Finally, at high temperatures, the chains begin to disappear. The material chains are formed because the ammonium molybdate starts boiling upon reaching the substrate surface; the frantic movement of the drops persists until the water and the ammonium in the precursor solution evaporate. The evaporation process is very fast at high temperatures, and the drops cannot move much on the sample's surface; the drops' displacements are shorter, and the material chains begin to disappear. It is possible to observe, in some cases, some drops bursting on the substrate surface, generating very small-sized and flower-shaped material.

In Fig. 6, the surfaces are shown at high magnification. The samples prepared at a substrate temperature of 423 K have very small-diameter grains, so that no borders can be observed. Crystallite size remains constant between 473 K and 623 K, and the grains share a single border. At a substrate temperature of 673 K, the grains have different shapes, are independent from each other, and do not share the same border, and thus are surrounded by empty spaces.

3.3. *Optical Characterization*

The substrate temperature significantly affects the color of the sample. Samples prepared at a substrate temperature of 673 K show a green aquamarine color; if the temperature decreases to 573 K, the samples turn blue, and at 423 K they acquire a semi-opaque white color.

The physical system employed to obtain the material's optical constants is shown in Fig. 7. The MoO_3 thin film is supported by a substrate of semi-infinite thickness and transparence for the spectral region evaluated. The transmittance of this optical system is given by [9]:

$$T = \frac{n_2}{n_0}\frac{\left[(1+g_1)^2+h_1^2\right]\left[(1+g_2)^2+h_2^2\right]}{e^{2\propto_1}+\left(g_1^2+h_1^2\right)\left(g_2^2+h_2^2\right)e^{-2\propto_1}+C\cos\ 2\gamma_1+D\sin\ 2\gamma_1} \quad (1)$$

where:

$$g_1 = \frac{n_o^2-n_1^2-k_1^2}{(n_o+n_1)^2+k_1^2} \quad (2)$$

$$h_1 = \frac{2n_ok_1}{(n_o+n_1)^2+k_1^2} \quad (3)$$

$$h_2 = \frac{2(n_1k_2-n_2k_1)}{(n_1+n_2)^2+(k_1+k_2)} \quad (4)$$

$$g_2 = \frac{n_1^2-n_2^2+k_1^2-k_2^2}{(n_1+n_2)^2+(k_1+k_2)^2} \quad (5)$$

$$\propto_1 = \frac{2\pi k_1 d_1}{\lambda} \quad (6)$$

$$\gamma_1 = \frac{2\pi n_1 d_1}{\lambda} \quad (7)$$

$$C = 2(g_1g_2-h_1h_2) \quad (8)$$

$$D = 2(g_1h_2+h_1g_2) \quad (9)$$

$n_o=1$ is the air's refraction index, n_1 and k_1 the real and imaginary parts of the MoO_3 refraction index, and $n_2=1.52$ and $k_2=0$ the glass refraction index and extinction coefficient, respectively.

In Eq. (2), the real and imaginary parts of the material's refraction index are unknown; these values are obtained through the theoretical simulation of the experimental transmittance spectra, permanently comparing the theoretical spectrum with the experimental one in accordance with the equation:

$$T(n_1, k_1d_1, \lambda)-T_{exp} = 0. \quad (10)$$

When the curves overlap, the theoretical values of the sought optical constants are extracted. This procedure requires that the difference between the two spectra be smaller than 1%. The thickness of the sample is included in the calculation as a known parameter.

Initially, in the calculation it is assumed that $k_1=0$ in the sample's most transparent region, and approximated n_1 values are determined; then, with these n_1 values, k_1 values are calculated. This procedure is repeated until the difference between the spectra does not change appreciably.

Fig. 8 shows the transmittance spectra obtained for samples prepared at different substrate temperatures. The spectra reveal the existence of light absorption in the entire region. For wavelengths shorter than 400 nm, there is a strong absorption zone related to light absorption due to band-to-band transitions in the material. There is a strong dependence of the transmittance curve on the substrate temperature for wavelengths longer than 600 nm. Samples prepared at a substrate temperature of 423 K are semi-transparent, with 92% transmittance; the samples' transmittance decreases considerably when the substrate temperature increases.

The spectral variations for the refraction index and for the extinction coefficient were determined from the theoretical simulation of the experimental transmittance spectra. The

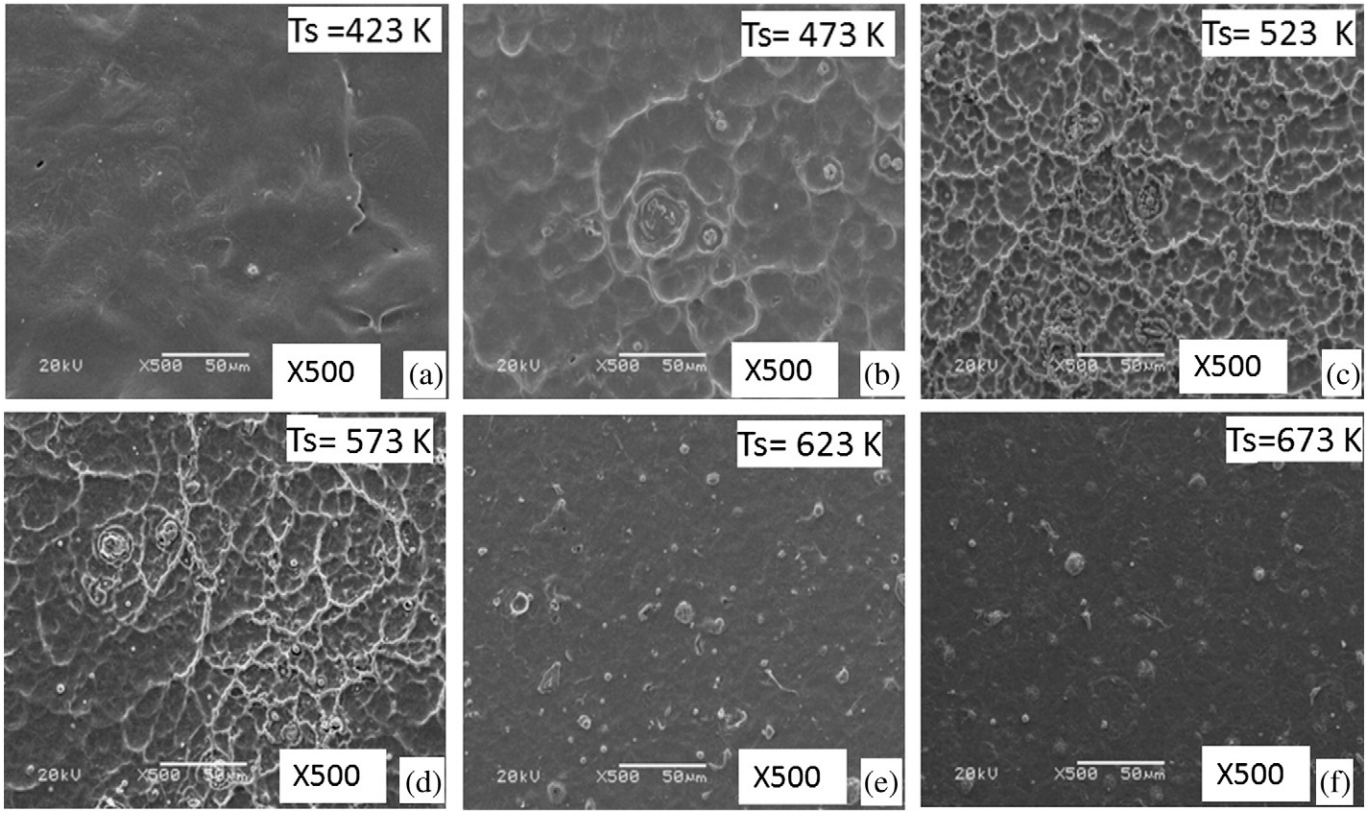

Fig. 5 – Micrographs of films obtained at different substrate temperatures. Magnification 500×.

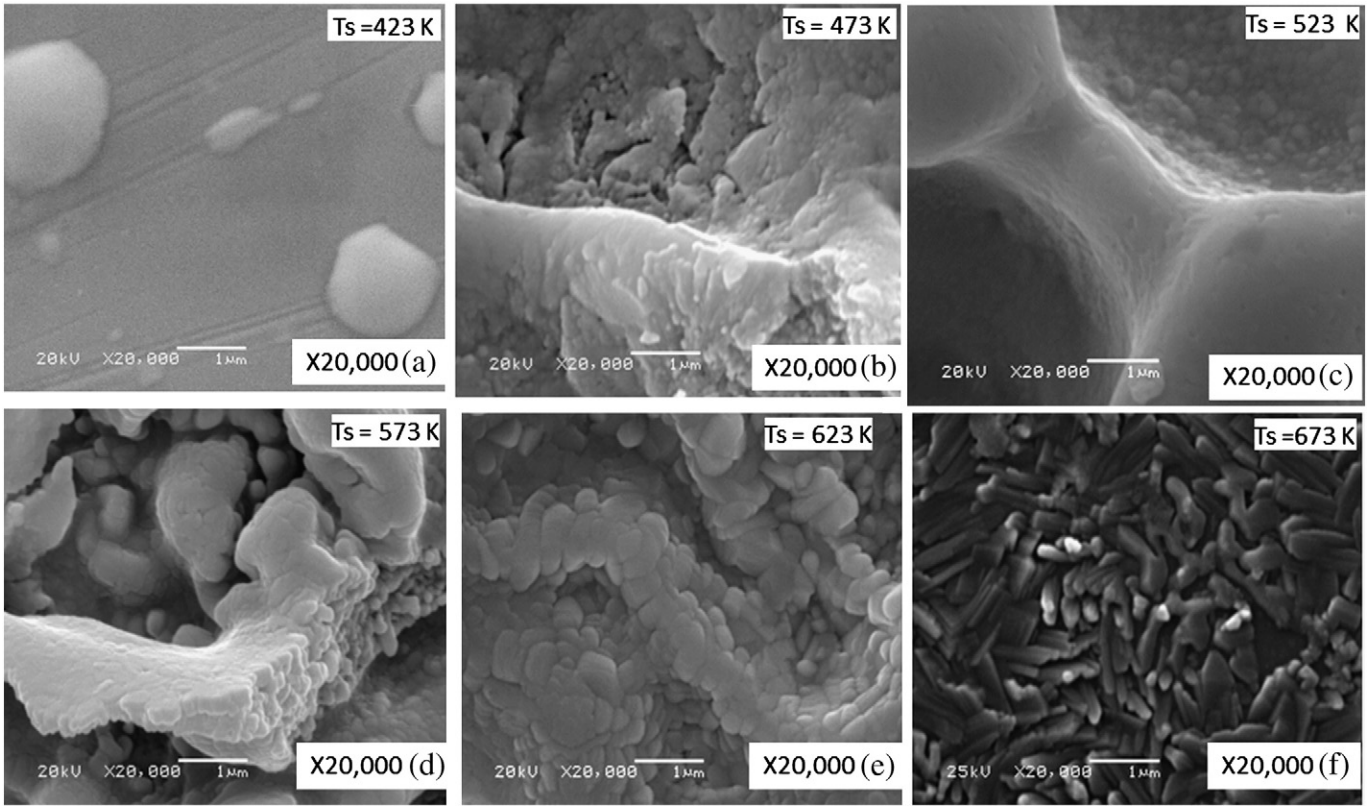

Fig. 6 – Micrographs of films obtained at different substrate temperatures. Magnification 20,000×.

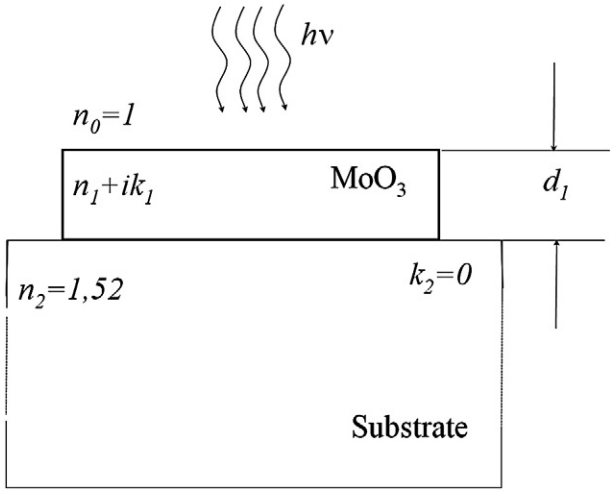

Fig. 7 – Physical system used to simulate the experimental transmittance spectra. The MoO_3 thin film is supported by a substrate of semi-infinite thickness.

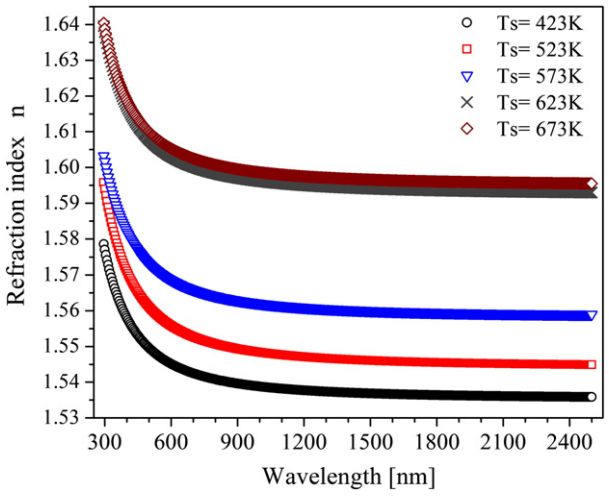

Fig. 9 – Refraction index for films obtained at different substrate temperatures.

extinction coefficient allowed determining the absorption coefficient, and from this the material's gap. Fig. 8 shows experimental spectra together with the theoretically simulated ones for different samples. It can be noted in this figure that in the entire region the experimental spectrum coincides with the theoretical one.

Fig. 9 shows the spectral variation for the refraction index obtained in the prepared samples. The index value for the samples prepared at a substrate temperature of 423 K was 1.6 (λ = 650 nm). The refraction index increases with the substrate temperature; these changes coincide with the samples' apparent changes of color described at the beginning of this section. Some authors have found an index between 1.6 and 2.0 for the same wavelength [10].

Fig. 10 shows the spectral variation of the absorption coefficients obtained for the different samples. In the high absorption region, high values, around 10^4 cm^{-1}, are obtained; these values are associated with band-to-band transitions in the material. A low absorption zone appears in the samples for wavelengths larger than 400 nm; this low absorption may be associated with oxygen vacancies in the material [11].

This absorption band increases with the substrate temperature, but could not be thoroughly analyzed, because the examined spectral region was too narrow. In this region, the sample's absorption increases with the substrate temperature.

The optical gap of the material was determined through the relation $(\alpha h\nu) = A_n(h\nu - E_g)^{1/2}$, where E_g is the forbidden energy gap and $h\nu$ the impinging photon energy. Fig. 11 shows the variation of $(\alpha h\nu)^2$ with $h\nu$ for films obtained at different substrate temperatures, as well as details of the calculation of the gap. The obtained gap's values are shown in Table 3 and compared with some gap values obtained by other authors. When the substrate temperature rises, the gap decreases. Samples prepared at substrate temperatures between 473 and 673 K crystallize in the MoO_3 orthorhombic phase, and the gap values should be the same for each sample, but it can be seen in the figure that an intense and wide absorption band exists in the low absorption region. This absorption became more

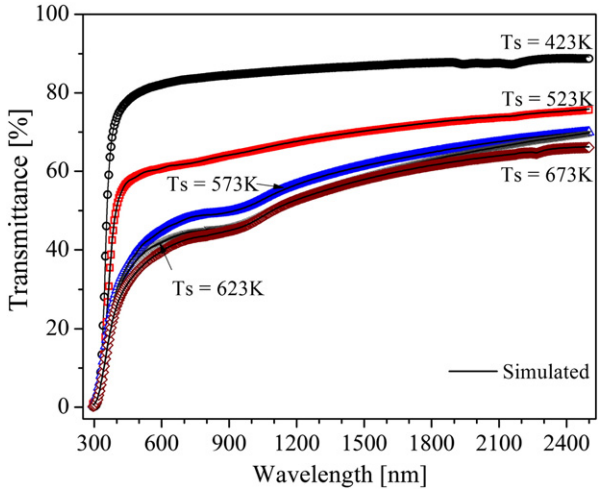

Fig. 8 – Experimental transmittance spectra of MoO_3 films obtained at different substrate temperatures.

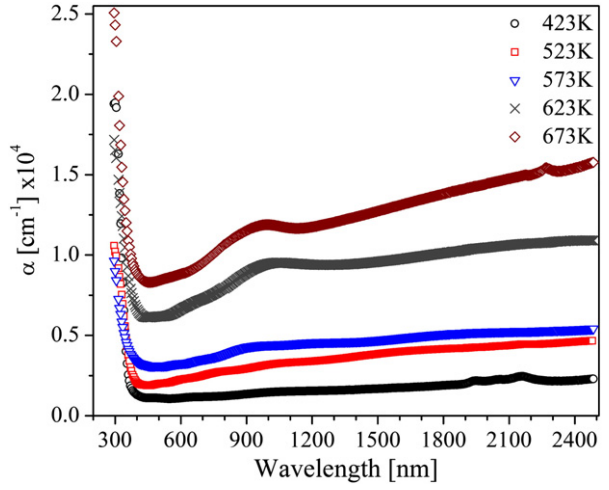

Fig. 10 – Absorption coefficient as a function of the wavelength for films obtained at different substrate temperature.

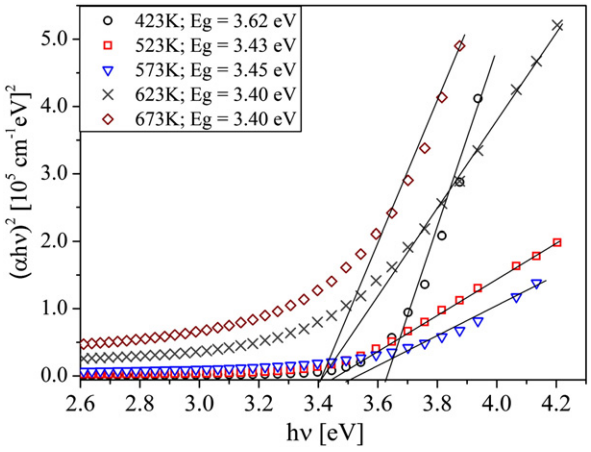

Fig. 11 – Relation between $(\alpha h\nu)^2$ and $h\nu$ for films obtained at different substrate temperatures.

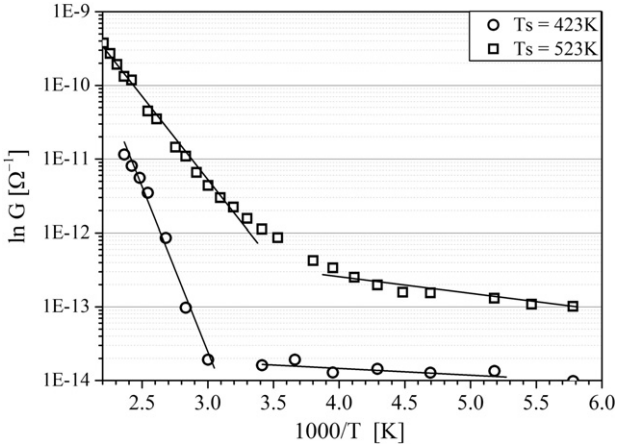

Fig. 12 – MoO_3 films electric conductance as a function of temperature.

intense and wide as the substrate temperature increased. Fig. 10 shows that this absorption band affects the position of the material gap. It is not possible to determine the exact position of the maximum absorption band, due to the shortness of the analyzed spectral region. This absorption band may be associated with oxygen vacancies in the material [11]. Bouzidi [3] obtained 3.14 eV in samples prepared by spray pyrolysis at substrate temperature of 573 K, and he also observed the same tendency in the change of the gap's values with substrate temperature. Finally, it is possible to associate a gap value of 3.62 eV with the specie MoO_3 $(H_2O)_2$.

3.4. *Electrical Characterization*

The voltage applied between the electrodes was varied in the interval ±10 V; these curves are reproducible with a maximum relative percentage variation of 2%. In all cases, within the voltage range used the observed behavior was ohmic. The DC electrical conductance (G) measurements showed that sample prepared at a substrate temperature of 423 K has a room temperature conductance of around 10^{-14} ohm^{-1}; the conductance is higher by an order of two magnitudes in the sample prepared at 523 K. Fig. 12 shows the plot log G vs. 1000/T for the two samples. The conductivity increases exponentially with increasing temperature. The curves suggest that two transport mechanisms exist in both samples. Two activation energy values were found for each sample. In the sample prepared at 423 K, substrate temperature 0.9 eV between 300 and 400 K and 0.02 eV for temperatures lower than 200 K were found. For the sample prepared at 523 K, 0.44 eV between 300 and 473 K, and 0.05 for temperatures lower than 200 K were found. Those values indicate that the electrical conduction in the samples is due to the band-to-band transitions or intrinsic conductivity for high temperatures and hopping for low temperature [15]. At low temperature, the conductivity obeys Mott's relation. The hopping conductivity may be attributable to the formation of a large number of oxygen ion vacancies in the samples.

Table 3 – Gap energy values obtained on the samples prepared at different substrate temperature.

Substrate temperature [K]	Gap [eV]
423	3.62
523	3.43
573	3.45
623	3.40
673	3.40
473 to 573	3.3 to 3.14 [3]
473 to 523	3.7 to 3.0 [12]
313 to 523	3.24 to 2.98 [11]
473	3.36 to 3.13 [13]

The following procedure was applied to study the effect of the MoO_3 films' exposure to CO and to H_2O: the sample was placed in a high-vacuum system that operated at a base pressure of 2×10^{-4} Pa. Keeping the first sample at 423 K and the second sample at 523 K, the gas (CO or H_2O) was introduced into the system until it reached a pressure of 1×10^{-2} Pa. The sample was cooled to 100 K. From this point on, the temperature of the sample was increased in a controlled manner, and the I–V curves were taken. In both cases, the films' resistance decreased with respect to its value in a vacuum, which indicates that the adsorption of these gases has a reduction effect. This result also agrees with theoretical results obtained from first principles calculations [14]. Actually, these studies show that the O atom in the H_2O molecule and the C atom in the CO molecule link to the surface through one of the O atoms in the MoO_3. Charge distribution calculations in systems H_2O/MoO_3 and CO/MoO_3 clearly reveal that there is a net charge transfer from the adsorbent gas molecules towards the MoO_3 molecules. This charge transfer, though small, is much more pronounced in the H_2O adsorption than in that of CO. This result is also consistent with the measured films' sensitivity in both cases. These curves are displayed in Figs. 13 and 14. At room temperature, the sensitivity of the films to CO varies between 15% and 45%, depending on the crystallographic structure, being greater in those films with a predominant alpha phase. Likewise, the films' sensitivity to H_2O varies between 40% and 85%.

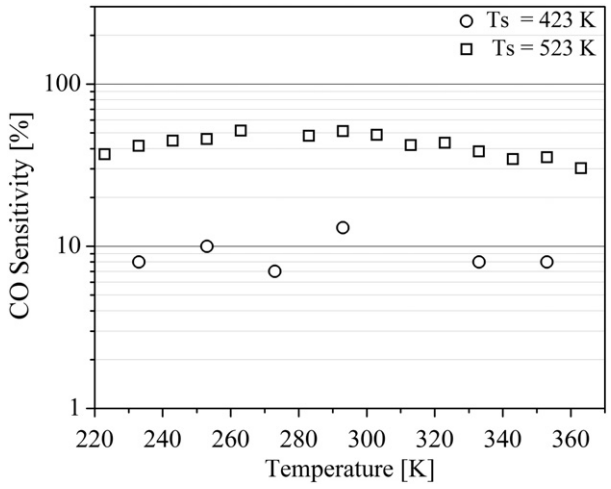

Fig. 13 – MoO_3 films sensitivity to CO as a function of temperature.

4. Conclusions

Good-quality MoO_3 thin films were prepared through the spray pyrolysis technique from tetra-hydrated ammonium hepta-molybdate onto Corning glass substrates maintained at temperatures between 423 and 673 K. Micro Raman and XRD analysis confirmed that samples prepared at 423 K were MoO_3 $(H_2O)_2$; as the substrate temperature rise, the water evaporates and the samples crystallize entirely in the a-MoO_3 phase. Good crystalline material was obtained in samples prepared at 673 K. Films prepared at low substrate temperature showed gap values of 3.62 eV, which decreased to 3.4 eV in samples prepared at 673 K. Electrical measurements showed two transport mechanisms components: electron hopping conduction occurring below 200 K and intrinsic conduction mechanism for temperatures over 200 K. The variation in the gap values and the conduction through the hopping mechanism can be attributed to the formation of a large number of oxygen vacancies in the samples. The samples prepared at 523 K substrate temperatures showed higher sensitivity to CO, while those prepared at 423 K showed higher sensitivity to water vapors.

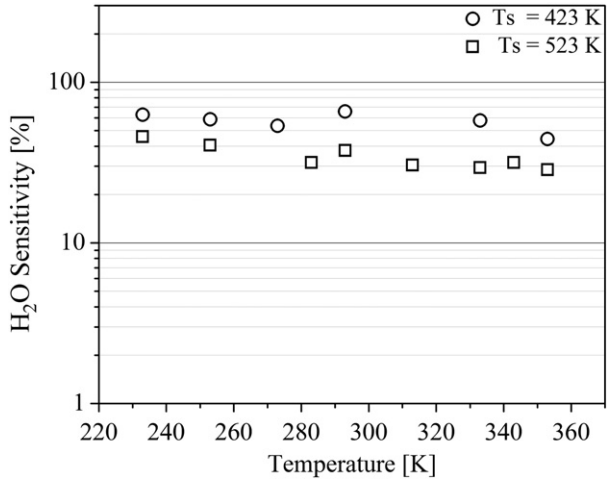

Fig. 14 – MoO_3 films sensitivity to H_2O as a function of temperature.

Acknowledgments

The authors wish to thank the DIB of the Universidad Nacional de Colombia, Antonieta Mondragón, Alicia del Real and Beatriz Millan Malo Departamento de Nanotecnología, Centro de Física Aplicada y Tecnología Avanzada, Universidad Nacional Autónoma de México, Juriquilla Campus, Querétaro, Qro, México.

REFERENCES

[1] Yang WQ, Wei ZR, Zhu XH, Yang DY. Strong Influence of substrate temperature on the growth of nanocrystalline MoO_3 thin films. Phys Lett A 2009;373:3965-8.
[2] Imawan C, Steffes H, Solzbacher F, Obermeier E. A new preparation method for sputtered MoO_3 multilayer for applications in gas sensors. Sens Actuators B 2001;78: 119-25.
[3] Bouzidi A, Benramdane N, Tabet-Derraz H, Mathieu C, Khelifa B, Desfeux R. Effect of substrate temperature on the structural and optical properties of MoO_3 thin films prepared by spray pyrolysis technique. Mater Sci Eng B 2003;97:5-8.
[4] Itoh T, Matsubara I, Shin W, Izu N, Nishibori M. Preparation of layered organic–inorganic nanohibrid thin films of molybdenum trioxide with polyaniline derivatives for aldehyde gases sensors of several tens ppb level. Sens Actuators B 2008;128:512-20.
[5] Kaur J, Vankar VD, Bhatnagar MC. Effect of MoO_3 addition on the NO_2 sensing properties of SnO_2 thin films. Sens Actuators B 2008;133:650-5.
[6] Seguin L, Figlarz M, Cavagnat R, Lasségues JC. Infrared and Raman spectra of MoO_3 molybdenum trioxides and $MoO_3{\cdot}xH_2O$ molybdenum trioxide hydrates. Spectrochim Acta A 1995;51:1323-44.
[7] Haro-Poniatowski E, Jouanne M, Morhange JF, Julien C, Diamant R, Fernamdez-Guasti M, et al. Micro-Raman characterization of WO_3 and MoO_3 thin films obtained by pulsed laser irradiation. Appl Surf Sci 1998;127–29:674-8.
[8] Oyerinde OF, Weeks CL, Anbar AD, Spiro TG. Solution structure of molybdic acid from Raman spectroscopy and DFT analysis. Inorg Chim Acta 2008;361:1000-7.
[9] Heavens OS. Optical Properties of Thin Solid Films. Dover Publications INC.; 1991. p. 77.
[10] Mondragón MN, O. Zelaya, Ramírez-Bon R, Herrera JL, Reyes-Betanzo C. Refraction index and oscillator strength in MoO_3, photocolored films. Physica B 1999;271:369-73.
[11] Sabhapathi VK, Hussain OM, Uthanna S, Naidu BS, Reddy PJ, Julien C. A.c. conductivity studies on A1/MoO_3/A1 sandwich structures. Mater Sci Eng B 1995;32:93-7.
[12] Yahaya M, Salleh MM, Talib IA. Optical properties of MoO_3 thin films for electrochromic windows. Solid State Ionics 1998;113–115:421-3.
[13] Tarsame SS, Reddy GB. Optical, structural and photoelectron spectroscopic studies on amorphous and crystalline molybdenum oxide thin films. Sol Energy Mater Sol Cells 2004;82:375-86.
[14] Sayede AD, Amriou T, Pernisek M, Khelifa B, Mathieu C. An ab initio LAPW study of the α and β phases of bulk molybdenum trioxide, MoO_3. Chem Phys 2005;316:72-8.
[15] Mott NF, Davis EA. Electronic processes in non crystalline materials. Oxford: Clarendon; 1971. p. 213.